3.1 A NOVEL TRAJECTORY ENSEMBLE MODEL OF STRATIFORM CLOUD AND ITS POSSIBLE APPLICATIONS

M. Pinsky(1), A. Khain*(1), L. Margariz (1), N. BenMoshe(1), A. Sterkin(2), O. Krasnov (3) and H. W. J. Russchenberg (3)

(1) The Hebrew University of Jerusalem, The Institute of the Earth Science, Israel
(2) Weizman Institute of Sciences, Rechovot, Israel
(3) International Research Centre for Telecommunications-transmission and Radar, Faculty of Information Technology and Systems, Delft University of Technology, Netherland

1. INTRODUCTION

Warm stratiform and stratocumulus clouds cover enormous areas of the Earth and play a crucial role in the radiative balance of the Earth affecting the climate and climatic changes, and contribute significantly to precipitation (see reference list) . The radiative properties of clouds strongly depend on the shape of droplet size distributions (DSD), (e.g.,Twomey, 1977; Feingold et al, 1994), so that small changes in DSD can lead to significant changes of the radiation balance. Important factors influencing DSD are the concentration and size distribution of atmospheric aerosol particles (AP), including the anthropogenic ones. An increase of the AP concentration leads to a larger number of cloud droplets. The resulting clouds reflect more solar radiation, the so called first indirect aerosol effect (Twomey, 1997; Sekiguchi et al 2002). Especially strong changes of DSD and cloud coverage are related to drizzle formation (e.g., Stevens et al 1998; vanZanten et al, 2005; Petters et al 2005). At the same time mechanisms of DSD and drizzle formation in stratocumulus clouds are still not well understood.

**Corresponding author address:* Alexander P. Khain, The Hebrew Univ. of Jerusalem, Israel, Depart. Atmospheric Sciences, e-mail:
khain@vms.huji.ac.il

Microphysical properties of stratiform clouds were measured by research aircraft in the course of several national and international field experiments: e.g., JASIN (Slingo et al 1982); Atlantic Stratocumulus Transition Experiment (ASTEX) (Martin et al, 1994; Albrecht et al, 1995; Duynkerke et al 1995; Frish et al 1995; Ramanathan et al 2001), First International Satellite Cloud Climatology Project (ISCCP) Regional Experiment (FIRE; Austin et al 1995); the second Aerosol Characterization Experiment (ACE-2; Brenguier et al, 2000a; Pawlowska et al, 2000). Using these data, many useful statistical results, such as relationships between aerosol concentration and cloud droplet concentration were found both form observed data and numerical simulations (e.g. Martin et al, 1994; Segal at al 2006), drizzle parameterizations were formulated for general circulation models (e.g. Khairoutdinov and Kogan 2000; Pawlowska and Brenguier 2003), dependences of drizzle formation on mean cloud depth and droplet concentration (e.g. Gerber 1996; Brenguier et al 2000b) were proposed.

At the same time fundamental mechanisms of DSD and drizzle formation in stratocumulus clouds are still not well understood. As is mentioned by Stevens et al (2003) " Although there exists a modest and growing literature on drizzle in the stratocumulus-topped boundary layer (STBL) some very elementary questions remain, including the actual precipitation rates in marine stratocumulus and their relation to ambient aerosol, cloud thickness, and intensity of turbulence".

This situation is related both to the lack of the theoretical understanding and appropriate observed data. It is well known that DSD are formed under a strong influence of the atmospheric boundary layer (ABL) dynamics. However, aircraft measurements of cloud microphysics were seldom accompanied by corresponding measurements of the dynamical (including turbulent) properties of the ABL. Even such important parameter as the velocity at the cloud base is often not measured. Respectively, state-of–the art numerical models produce dynamical structure of STBL by "themselves" using "large-scale" sounding as the only source of thermodynamic information.

Regular ground based Doppler radar measurements of the cloud topped BL dynamics have become recently available (e.g., LeMone, M.A., 1990, Fox and Illingworth, 1997: Kollias and Albrecht, 2000; Krasnov and Russchenberg 2002; Crewell et al, 2004; O'Connor et al, 2004; Russchenberg et al 2004, Wolf et al, 2000). The measurements of Doppler radars are performed with the interval of a few seconds, which provides detailed information about the wind fields within the whole BL. At the same time, synchronic measurements of the ABL dynamics and cloud microphysics remained quite rare. A unique data collected during recent the Dynamics and Chemistry of Marine Stratocumulus II field study (DYCOMPS-II) (Stevens et al 2003) contain both microphysical and Doppler radar measurements, which allows one to fill many gaps mentioned above. In particular the data contains turbulent characteristics such as magnitudes and vertical profiles of vertical velocity variance $\sigma_w^2 = \langle W'^2 \rangle$ (Stevens et al 2005; Lothon et al 2004).

The in situ measured drizzle fluxes turned out to be highly non-uniform in the horizontal with several characteristic scales (mainly ~10 km and ~1km) (VanZanten et al 2005) in spite of the relatively homogeneous cloud structure. A high correlation of enhanced drizzle was found thought the CTBL depth, from cloud top to the surface. It was found that drizzle was much more prevalent in clouds having effective radius of exceeding about 8.5 μm (VanZanten et al, 2005; Twohy et al 2005), which agrees with results of Yum and Hudson (2002) and is significantly smaller than 15-16 μm found by Gerber (1996) for heavy drizzle formation and by Rosenfeld and Gutman (1994) and Pinsky and Khain (2002) for triggering the raindrop formation in cumulus clouds.

Numerical modeling is a potentially efficient tool for investigation of physical mechanisms responsible for these (and other) effects. The models could serve as a connecting link between the dynamical properties of the BL, cloud microphysics and cloud radiative properties. Large eddy simulation (LES) models have emerged as a powerful tool to simulate the microphysical properties of stratocumulus clouds (e.g., Kogan et al, 1994; Feingold et al, 1994, 1998a,b; Stevens et al, 1996, 1999; Moeng et al 1996; Khairoutdinov and Kogan, 1999; Khairoutdinov and Randall 2003). The LES models are usually regarded to as models that are rich in dynamics, but not so rich in microphysics (Feingold et al, 1998b). These models usually contain simplified parameterizations of microphysical processes, for instance, those of droplet nucleation and denucleation (release of solid AP by droplet evaporation). As a rule, the LES models have problems with the proper representation of successive AP growth as a result of the nucleation-collision-evaporation droplet chain. The LES models use a fixed mass grid to represent the DSD that often leads to an artificial droplet spectrum broadening. In the state-of-the-art LES models turbulence (in its parameterized form) plays the role of friction (or filtering) and cannot serve as a source of supersaturation fluctuations.

Recent intercomparison of ten state-of-the art very high resolution LES models was performed by Stevens et al (2005) to evaluate the fidelity with which LESs can represent the turbulent structure of STBL. The STBL turbulent structure observed during the first research flight (non-drizzling case) of DYCOMS-II was simulated. It seems that most of LESs significantly overestimate the entrainment rate at cloud top. This overestimation is caused by several reasons, including numerical viscosity and other problems related to representation of small-scale turbulence. Stevens et al (2005) conclude that "in the absence of significant leaps in the understanding of subgrid-scale physics, the appropriate representation of processes at cloud top can only be achieved by a significant refinement in resolution (up to 1 m)- a refinement that, while conceivable given existing resources, is probably still beyond the reach of most centers".

It was found that most of simulations tended to predict more broken cloud with a higher cloud base, and less liquid water than was observed. Most of the LESs were unable to predict such important characteristics of the STBL turbulent structure, for instance they significantly underestimate magnitudes of vertical velocity variance $\sigma_w^2 = \left\langle W'^2 \right\rangle$ and highly overestimate the skewness $\left\langle W'^3 \right\rangle$ within cloud layer, and especially in the vicinity of cloud top. Since dynamic/turbulent structure of the STBL is caused by many factors such as radiation, heat fluxes from the surface, thermal instability, latent heat release, small-scale turbulence in zones of different temperature gradients, it is not wonder that even small errors in representation of any of these processes can affect model dynamics, that it its turn affects the cloud microphysical structure. In particular, according to Stevens et al (2005) most of LES models tested underestimated the values of liquid water content.

These conclusions indicate the necessity to look for other approaches allowing accurate simulation and analysis of cloud microphysical processes, might be, at the expense of utilization of less general and more idealized approaches as compared to the LES models. In this study we propose an approach representing a further development of trajectory ensemble models (TEM). The microphysical cloud structure will be simulated using the turbulent-like ABL dynamics with observed energetic and statistical (correlation) properties. The purpose of this study is to investigate processes of the formation and spatial variability DSD at small time and spatial scales under a given dynamical structure of the STBL typical of both non-drizzling and drizzling clouds. We are going to reproduce the classical concept of the formation of stratocumulus clouds, as a result of air mixing by eddies of different scales in the ABL. As a result of such stirring, stratification in the subcloud and cloud layers should tend to dry and moist adiabat, respectively (e.g., Garratt, 2000; Stevens 2003b). Among the questions we address in this study are: a) what are the processes determining the shape and spatial variability of DSD; b) How does drizzle form in stratocumulus?

2. MODEL DESCRIPTION

2.1 Concept of the model

To address the questions mentioned above it is desirable to use the Lagrangian approach known as rich in microphysics (mainly, in the representation of diffusion droplet growth/evaporation). This approach is usually used either in single-parcel models (Bower and Choularton, 1993; Pinsky and Khain, 2002) or in trajectory ensemble models (TEM) (e.g., Stevens et al 1996; Feingold et al, 1998b; Harrington et al 2000; Erlick et al, 2005). The advantage of these models, from the microphysical point of view, is that they solve the equation of aerosol particles and droplet growth on a variable mass grid. This eliminates arbitrary distinction between aerosol particles (AP) and droplets, and a continuous AP growth is allowed; for instance, Pinsky and Khain (2002) used a 2000-bin variable mass grid Lagrangian parcel model to simulate the process of AP growth and their transformation into droplets, without utilizing parameterization procedures of the in-cloud nucleation and de-nucleation (regeneration of AP following droplet evaporation). The utilization of variable mass grid eliminates artificial DSD broadening caused by the necessity of DSD remapping on the regular mass grid (e.g. Khain et al 2000). The TEM models usually consist of two sub-models: the LES model that is used to simulate the dynamics, and the Lagrangian parcel model. In these models droplet spectra are calculated in several hundred of Lagrangian cloud parcels moving within the velocity field calculated by a LES model. The microphysical properties of stratiform clouds are determined by the statistical analysis of the DSD formed in these individual parcels. This approach allows one to simulate DSD formation in parcels having different histories and to investigate reasons of the DSD variability.

Note that in the state-of-the art TEM cloud parcels are separated by significant distances. Respectively, drop sedimentation (exchange of droplets between individual parcels) is not taken into account. It means that the TEM can be applied only for the investigation of the DSD formation by the droplet diffusion growth when droplet collisions are ineffective (no drizzle formation). This limits the time of parcel motion simulations by several tens of minutes (Feingold et al 1998b; Harrington et al, 2000). The trajectories of Lagrangian parcels in the TEM are usually calculated only above the cloud base determined by the LES model. Thus, the TEM models cannot be used to investigate the interaction of cloud and subcloud layers, as well as aerosol recycling related to drop evaporation below the cloud base and new drop formation during successive air parcel ascent.

In the present study we describe a new TEM model that, as we believe, is as accurate as is necessary to attribute all model results to physical mechanisms, but not to numerically-induced effects. The scheme of physical processes described by the model is shown in **Figure 1**.

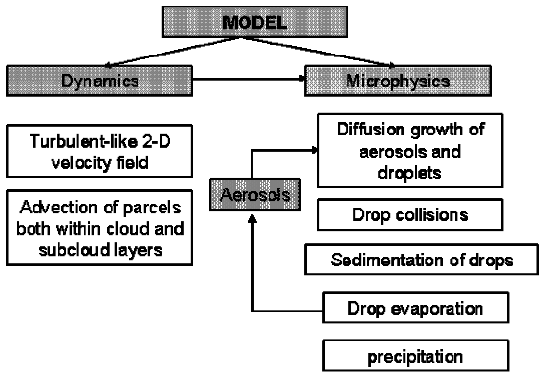

Figure 1. *The scheme of physical processes described by the model*

The specific feature of the new TEM is that Largrangian air parcels cover the whole BL area as it is shown schematically in **Figure 2.**

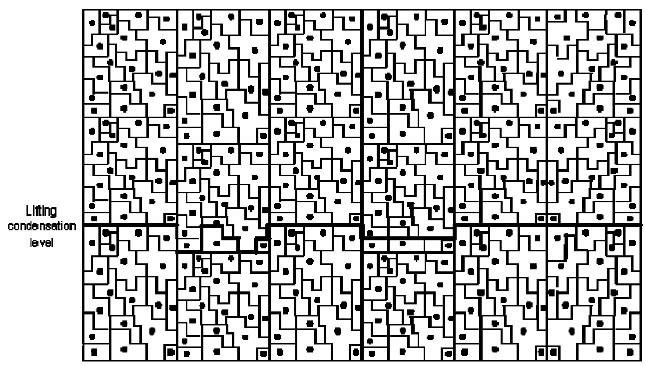

Figure 2*. Schematic location of Largangian air parcels within a computational area: in the model the parcels cover the whole BL area. Dots determine the coordinates that parcels are assigned. The number*

of air parcels is equal to 1840 in the current model version.

The parcels can be both droplet-free and cloudy. The latter contrasts with the state-of-the art TEM, where Lagrangian parcels are only cloudy ones and are separated by significant distances. At t=0 air parcels are distributed randomly over the whole area of the BL and contain non-activated AP only**.**

The parcels are advected by the time dependent flow that is generated by a model of turbulent-like flow. The velocity field has preset statistical properties, which can be derived from the radar data observed (see Appendix 1). The model of turbulent-like flow describes also large eddies with characteristic scales up the scale of ABL depth. Such eddies are typical of STBL. Respectively, the model is able to describe dynamics of the BL typical of both pure stratiform clouds and stratocumulus clouds.

In ascending parcels crossing the lifting condensation level some fraction of aerosols activates and gives rise to droplet formation. Thus, there exist non-activated aerosols and droplets in each cloud parcel. In the course of parcel motion supersaturation in parcels can be replaced by undersaturation, for instance in downdrafts, and droplets can evaporate partially or totally (denucleation). In the latter case the cloud parcel turns out to be a droplet-free parcel containing only wet aerosol particles. Besides, the parcels also transport potential temperature and humidity. In this way the model reproduces interaction between the subcloud and cloud layers.

The new model takes into account collision between droplets in each parcel and droplet sedimentation. This allows simulation of drizzle formation and fall down to the surface.

As it was mentioned above, the cloud is simulated under a *given* turbulent-like ABL dynamics with characteristic energetic, time and spatial correlation properties (see below for details). In the present study these properties are assumed unchangeable during simulations. We see the justification of this simplification in the following. The structure of stratocumulus clouds is affected by mechanisms of quite different time and spatial scales. For instance such factors as surface fluxes, radiation cooling, entrainment, mean vertical velocities, etc., have longer characteristic time scales (determined by synoptic situation) than the time scale of the ABL mixing by large eddies (Stevens et al 2003a). For instance, the cloud depth changes with the rate of a few m/hour (Stevens et al, 2003b). The mean entrainment rate found in the research flights in DYCOMS-II did not exceed as a rule about 0.5 cm/s, mean vertical velocity was of the same order of the magnitude (Stevens et al 2003b, 2005). At the same time the standard deviation of the vertical velocity related to large eddies and turbulent fluctuations is of ~0.6-0.8 m/s (Stevens et al 2005). The eddy turnover times (as measured by the ratio between the PBL height and the convective velocity scale) are or order of 10 min (Stevens et al 2005). It means that droplet concentration, shape of droplet spectra, spatial variability of DSD and other microphysical properties are determined by processes with characteristic scales much smaller than those determining statistical properties of the PBL dynamics. Besides, the "macro-scale" factors influence largely the dynamic (turbulent) structure of the BL that in its turn, affects the cloud microphysical structure. Our idea was to simulate cloud formation under the influence of the ABL dynamics observed. We believe that the turbulent-like structure of the BL adapts rapidly to the environmental situation. Respectively, this structure can be considered unchanged at time scales smaller than the "environmental" time scale.

We did not take into account the effects of latent heat release on the dynamic (turbulent) structure explicitly. Instead, we generate the turbulent-like dynamical structure that corresponds to that observed in the STBL. This dynamical structure is formed under a combined effect of latent heat release, entrainment, surface fluxes, etc. We believe that the microphysical structure of clouds should correspond to the ABL dynamics. Simulation of turbulent-like flows corresponding to different thermodynamic situations in the STBL makes it possible to investigate the effects of the ABL dynamics and aerosol properties on the microphysical structure of stratocumulus clouds.

Yet, in this study we do not take into account the possible effects of drizzle on ABL dynamics that can be accompanied by the formation of open-cell-like features (pocket of open cells) (e.g. VanZanten and Stevens 2005b). Note first that drizzle can exist without significant changes of the ABL dynamics (VanZanten et al 2005a). Microphysical properties of clouds forming pockets of the open cells can be investigated within the frame of our approach by utilization of the corresponding ABL dynamics.

In spite of obvious limitations of this simplified approach, we believe that the model allows one to reproduce realistically the process of cloud microphysical structure formation at time scales of several turnover times and spatial scales of a few kilometers.

2.2 Model dynamics

Motion equations. The velocity field in the BL caused by eddies of different nature and small-scale turbulence is represented as the sum of a great number of harmonics including those representing large eddies with scales of the ABL depth. The mean horizontal velocity $V_0(z)$ is also taken into account. As shown below the statistics of the velocity field can be tuned to the observations. The expressions for the vertical $W(x,z,t)$ and the horizontal $V(x,z,t)$ velocity components are as follows:

$$W(x,z,t) = \sum_{m=1}^{M}\sum_{n=1}^{N} C_n D_m \left[a_m(t)\sin\frac{2\pi mx}{L} + b_m(t)\cos\frac{2\pi mx}{L} \right] \sin\frac{\pi nz}{H} \quad (1a)$$

$$V(x,z,t) = \sum_{m=1}^{M}\sum_{n=1}^{N} C_n D_m \frac{n}{m}\frac{L}{2H} \left[a_m(t)\cos\frac{2\pi mx}{L} - b_m(t)\sin\frac{2\pi mx}{L} \right] \cos\frac{\pi nz}{H} + V_0(z) \quad (1b)$$

where C_n, D_m are the coefficients described below, M and N are the numbers of harmonics in the horizontal and the vertical directions, respectively; *L* and H are the sizes of the computational area in the horizontal and vertical directions, respectively.

Random fluctuations of the velocity field with time are represented by independent auto regression series of the first order $a_m(t)$ and $b_m(t)$:

$$a_m(t+1) = \vartheta_m a_m(t) + \sqrt{1-\vartheta_m^2}\,\varepsilon_m(t+1)$$

$$b_m(t+1) = \vartheta_m b_m(t) + \sqrt{1-\vartheta_m^2}\,\eta_m(t+1) \quad (2)$$

where ϑ_m are the parameters determining the characteristic correlation time of velocity harmonics having corresponding wave lengths; ε_m and η_m are normal white noise with zero mean values and unit variation.

The correlation functions $R_m(\tau)$ of autoregression sequences (2) are exponents $R_m(\tau) = \exp(-\tau/\gamma_m)$ with the characteristic correlation time $\gamma_m = -(\ln\vartheta_m)^{-1}$.

Coefficients $a_m(t)$ and $b_m(t)$ obey the following conditions:

$$\langle a_m(t)\rangle = \langle b_m(t)\rangle = 0$$

$$\left\langle a_m(t)a_j(t)\right\rangle = \left\langle b_m(t)b_j(t)\right\rangle = \delta_{mj}$$
$$\left\langle a_m(t)b_j(t)\right\rangle = 0 \qquad (3)$$

,

where δ_{mj} is the Kronecker symbol. The velocity field (1a-1b) has the following properties:

a) It obeys the continuity equation: $\frac{\partial W}{\partial z} + \frac{\partial V}{\partial x} = 0$;

b) The vertical velocities at the upper (z=H) and lower (z=0) boundaries are equal to zero $W(x,0,t) = W(x,H,t) = 0$. The conditions are widely used in numerical and analytical studies, which in our case do not allow parcels to leave the BL:

c) Cyclic lateral boundary conditions: $W(x,z,t) = W(x+L,z,t); V(x,z,t) = V(x+L,z,t)$

d) Average values with respect of a great number of realizations are equal to those averaged with respect to the horizontal direction:

$\left\langle W(x,z,t)\right\rangle = 0; \left\langle V(x,z,t)\right\rangle = V_0(z)$.

The energetic and correlation characteristics of the velocity field given in (1) are as follows.

a) Velocity variations can be expressed as (see Appendix):

$$\left\langle W^2\right\rangle = \sum_{m=1}^{M} D_m^2 \left[\sum_{n=1}^{N} C_n \sin\frac{\pi nz}{H}\right]^2$$

$$\left\langle (V-V_0)^2\right\rangle = \left(\frac{L}{2H}\right)^2 \sum_{m=1}^{M}\left(\frac{D_m}{m}\right)^2{}^2$$
$$\left[\sum_{n=1}^{N} nC_n \cos\frac{\pi nz}{H}\right] \qquad (4)$$

where $\sum_{m=1}^{M} D_m^2 = 1$. The variations depend only on the vertical coordinate z. The values averaged with respect a great number of realizations are equal to the horizontally averaged values because of the cyclic boundary conditions.

b) The correlation functions along the horizontal direction are given as (see Appendix):

$$B_W(\Delta x, z) = \left[\sum_{n=1}^{N} C_n \sin\frac{\pi nz}{H}\right]^2 \sum_{m=1}^{M} D_m^2 \cos\frac{2\pi m\Delta x}{L}$$

(5)

$$B_V(\Delta x, z) = \left(\frac{L}{2H}\right)^2 \left[\sum_{n=1}^{N} nC_n \cos\frac{\pi nz}{H}\right]^2$$
$$\sum_{m=1}^{M}\left(\frac{D_m}{m}\right)^2 \cos\frac{2\pi m\Delta x}{L}$$

The correlation functions depend only on $\Delta x = x_2 - x_1$. Again, averaging over a great number of realizations is equivalent to averaging in the horizontal direction.

c) The cross- correlation functions of velocity components along the horizontal direction depend only on $\Delta x = x_2 - x_1$:

$$B_{VW}(x_1, x_2, z) = f(\Delta x, z)$$
$$B_{VW}(0, z) = 0 \qquad (6)$$

As a result, correlations between two velocity components in one and the same point are equal to zero. Thus, the field (1a,b) is stationary and uniform in the horizontal direction. The field obeys ergodic properties, namely: averaging with respect to realizations is equivalent to averaging along the horizontal direction.

Tuning of the model dynamics.

The dynamical structure of the BL is of turbulent nature that can hardly be exactly assimilated or reproduced by numerical models. It is reasonably assume, however, that the cloud microstructure and cloud geometry are determined by the general energetic and correlation properties of the velocity field, depending in particular on the meteorological situation. Such properties can be derived either from the measurements or from suitable theoretical results, including those obtained using the LES models.

There are several main parameters of the model (1-3) that determine the properties of the velocity field in the BL:

a) Observations (and LES models) usually allow one to calculate the vertical profile of the r.m.s vertical velocity deviation $\left\langle W^2 \right\rangle^{1/2}$, whose magnitude corresponds to the "dynamical" or "convective" regimes of the BL (e.g., Babb and Verlinde, 1999; Kollias and Albrecht, 2000; Stevens et al 2003a, 2005) and supposedly affects DSD structure and drizzle forming processes (Feingold et al, 1996; Stevens et al 2003b, 2005). The variation of the vertical velocity field (1a) is given in (4). To calculate C_n, the measured profile $\left\langle W^2 \right\rangle^{1/2}$ should be reflected anti-symmetrically for z<0, and expanded into the Furrier series within the interval [-H,H]. The coefficients of the series represent the values of C_n:

$$C_n = \frac{1}{H}\int_{-H}^{H} \left\langle W^2 \right\rangle^{1/2} \sin\frac{2\pi nz}{H} dz \qquad (7)$$

There are several empirical formulas for vertical profiles of $\left\langle W^2 \right\rangle$ (e.g., Lenschov et al 1980). For current simulations, we have used profile $\left\langle W^2 \right\rangle = 3.2 \cdot (z/H)^{2.2} (1 - 0.8z/H)^{1.4}$ shown in **Figure 3.**

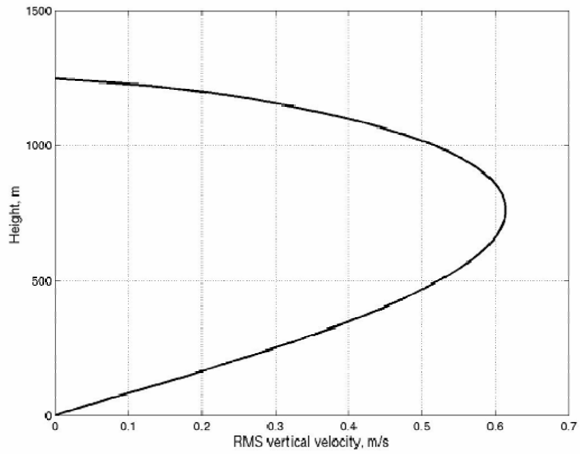

Figure 3. *Vertical profile of* $\left\langle W^2 \right\rangle^{1/2}$ *used in the simulations.*

The $\left\langle W^2 \right\rangle^{1/2}$ maximum of 0.6 m/s is located at 500 m. Note that this profile is quite similar to that observed in the second flight during which both weak and heavy drizzle was observed (VanZanten and Stevens 2005). In this study the “inversion” layer was taken somehow higher than that observed in DYCOMS-II.

b) The correlation properties of the velocity field determining the characteristic horizontal scale of velocity variation are determined by the correlation function of the vertical velocity in the horizontal direction. The shape of the correlation function is determined by coefficients D_m. In the present study D_m has been chosen in such a way that the correlation function $B_W(\Delta x, z)$ should meet the Kolmogorov theory:

$$B_W(\Delta x, z) = \left\langle W^2 \right\rangle \left(1 - \varepsilon^{2/3} \Delta x^{2/3}\right), \qquad (8)$$

where ε is the dissipation rate. The calculation of coefficients D_m was also performed using the expansion into the Fourier series.

c) The characteristic time scales of velocity fluctuations of different spatial scales are also subject to adaptation. In this study the characteristic time scales were assumed to meet the Kolmogorov relationships:

$$\gamma_n = \varepsilon^{-1/3}(H/n)^{2/3} \qquad (9)$$

d) One more additional parameter allowing the description of vortex structure in the model is the aspect ratio. It is reasonable that for small turbulent vortices this value is close to 1. The existence of LE usually indicates that convective instability (Emanuel 1994) or the inflection point instability (e.g. Faller and Keylor, 1966) take place in the BL. The typical aspect ratio for such eddies in the atmospheric BL is close to the critical value for vortexes formed as a result of the Rayleigh-Benard convective instability (e.g. Zhelnin and Khain 1975). Respectively, in this study the aspect ratio was chosen equal to L/2H =1.5. Sensitivity of results to the structure of large eddies will be investigated in future simulations.

e) The vertical velocity field (1) with correlation properties described above has zero skewness, which reflects the normality of the generated turbulent-like field. According to measurements during DYCOMS-II the magnitudes of skewness is quite close to zero at all heights in the STBL. At the same time, LES simulations predicted significant deviations of the skewness from zero (especially within the cloud layer) and significantly underestimate values of $\langle W^2 \rangle$ (Stevens 2003b, 2005). Thus, the velocity field we use in simulations has statistical properties that agree with observations better than those one can obtain using very high resolution LES models.

The main dynamical parameters of the current model version are presented in Table 1.

2.3 Model microphysics

The microphysics of a single Largangian parcel is described by Pinsky and Khain (2002) in detail. The microphysics of the parcel model includes the diffusion growth equation used for nuclei and water droplets

$$r\frac{dr}{dt} = \frac{1}{F}\left(S - \frac{A}{r} + \frac{Br_N^3}{r^3 - r_N^3}\right) \qquad (10)$$

where r and r_N are the droplet - and dry CCN radii, respectively. S is the supersaturation, A and B are the terms describing the effects of surface tension and chemical properties of aerosols, respectively (see Pruppacher and Klett, 1997 for more detail). The equation for supersaturation S is

$$\frac{dS}{dt} = (S+1)\left(A_1 W - A_2 \frac{dq}{dt}\right) \qquad (11)$$

where q is the liquid water content (LWC), A_1 and A_2 are the coefficients slightly depending on temperature. Vertical velocity W is adopted from the model dynamics.

Cloud particles (both non-activated nuclei and droplets) are described by the mass grid containing 500 mass bins within the 0.01 μm – 1000 μm radius range. The mass of each bin in the mass grid changes with time (height) according to the equation for diffusion growth. No special simplifying approach to distinguish non-activated CCN and droplets is applied. A small 0.01 s time step is used to calculate the diffusion growth of drops and nuclei. Such a small time step is necessary to simulate adequately the growth of the smallest AP, so that the separation between non-activated nuclei attaining equilibrium (haze particles) and the growing droplets is simulated explicitly (without parameterization) by solving the equation for the diffusion growth. The Lagrangian approach used eliminates the artificial spectrum broadening typical of models using two different immovable mass grids for dry AP and droplets, respectively.

The precise method proposed by Bott (1998) is used to solve the stochastic collision equation. Collision droplet growth was calculated using a collision efficiency table with a high 1 μm - resolution in droplet radii (Pinsky et al. 2001). Drop growth by collisions is calculated using a 1 s- time increment. Note that the microphysical equations are solved both in the subcloud and cloudy layers of the BL.

The location of parcels is determined by the coordinates of their "centers". Each parcel is characterized by the mass of water vapor, LWC and AP mass. In case of no sedimentation taken into account the parcels are adiabatic, i.e. the sum water vapor and LWC conserves both during advection and microphysical processes. This is an interesting limiting case, which, however, obeys many observations, at least in non-drizzling and weak drizzling CTBL. Thus, the mass and concentration are conserved both in each parcel and in the whole area. Droplet sedimentation changes LWC in each parcel, but does not change the total LWC (with the exception of the mass falling to the surface). The scheme illustrating the treatment of droplet sedimentation is illustrated in **Figure 4**.

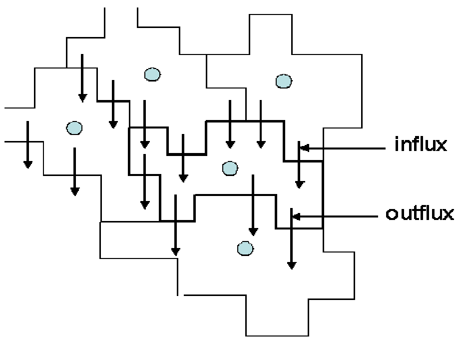

Figure 4. The scheme of calculation of droplet fluxes though the boundaries of adjacent parcels.

The interfaces between neighboring parcels are determined at each time step using a simple algorithm: each point between the centers of adjacent parcels is assigned to the parcel whose center is located closer. Each parcel boundary is described by a broken line consisting of 5 m-length straight line elements. The flux of radius-r droplets moving through the fraction of the parcel boundary with the length l_{ij} of the i-th parcel of square S_i is calculated as $\Delta N_i(r) = N_i \dfrac{l_{ij} V_{ti}(r)}{S_i} \Delta t$, where N_i and $V_t(r)$ are the concentration and fall velocity of droplets of radius r. The difference between influxes and outfluxes determines the changes of droplet concentration of r -radius droplets in the *i-th* parcel. This method actually represents an extension of the common procedure of particle sedimentation calculation used in the Eulerian models to the non-regular grid formed by centers of the parcels. The procedure conserves the sums of drop concentrations and drop masses in adjacent parcels for each bin.

Since the DSD evolution is different in different parcels, the mass assigned to bins in the mass grids of adjacent parcels can become different. Thus, in order to perform sedimentation, the DSDs of all parcels are interpolated into one and the same supplemental regular mass grid containing 500 bins. Such remapping conserves the mass and concentration of droplets and aerosols (including aerosols inside droplets). The remapping does not lead to the droplet spectrum broadening because of the high resolution of the supplemental mass grid.

The aerosol budget is calculated in the model. In cloudy parcels AP exist in two "states": a) non-activated wet AP (haze particles) and b) dissolved AP within droplets. Collisions of droplets are accompanied by the corresponding increase of the dissolved AP mass in drop-collectors. Evaporation of one drop gives rise to the release of one new AP (denucleation). Thus, size distribution of AP in parcels changes during their recirculation from the sub-cloud layer to the cloud layer and backwards.

The initial size distribution of AP in all parcels was represented by three mode log-normal distribution [Hobbs et al., 1985, Respondek et al., 1995; Segal et al, 2004]:

$$\frac{dN}{d\ln r_N} = \sum_{i=1}^{3} \frac{N_{0,i}}{\sqrt{2\pi}\log(\sigma_{N,i})\ln 10} \exp\left\{ - \frac{\left[\log(\frac{r_N}{R_i})\right]^2}{2(\log\sigma_{N,i})^2} \right\} \quad (12)$$

where R_i is the value of the aerosol radius at which i-th aerosol model is centered, $\sigma_{N,i}$ is the width of the i-th aerosol mode. Variation of parameters $N_{0,i}$, R_i and $\sigma_{N,i}$ allows one to simulate aerosol distributions within a wide range of conditions from very continental to very maritime ones (Philippin and Betterton, 1997; Martin et al. 1994; Elliott and Egami, 1975; Hudson, 1993; Segal et al 2004; Segal and Khain 2005). The minimum size of dry aerosol particles in the model is assumed equal to 0.01 μm. AP with radii below 0.01 μm hardly can be activated in stratiform clouds.

3. PRELIMINARY RESULTS

Preliminary simulations with the cloud topped BL model aim at verifying the ability of the model to simulate clouds with quite different microphysical structures, in particular, both non-drizzling and drizzling clouds. Note that in the present study we do not take into account the turbulent effects on droplet collisions.

The dynamical and microphysical parameters of the model used in these simulations are presented in **Table 1**.

Table 1. The main parameters used in preliminary simulations of cloud formation

Dynamic parameters		Microphysical and thermodynamical parameters	
Characteristic size of air parcels	~ 50 m	Number of mass bins	500
Number of parcels	1840	Range of cloud particles, μm	0.01-1000
Length of the area L, m	3750	Time step of diffusion growth, s	0.01
Height of the area H, m	1250	Time step for collisions, s	1.0
Number of harmonics M=N	50	Time step for sedimentation, s	1.0
Maximum r.m.s vertical velocity fluctuation, m/s	0.7	Number of modes in aerosol number distributions	3
Life time of harmonics, s	30-1000	Chemical composition of aerosols	NaCl
Time period of velocity field updating (eq. 2), s	0.1	Surface temperature, K	293.5
Turbulent dissipation rate, cm^2/s^3	10	Initial temperature gradient, C/km	9.8

Two simulations referred to as ND (no-drizzle) and D (drizzle) were carried out. The ridged upper boundary is identified with the temperature inversion at z= 1250 m. The only difference between the conditions of ND- and D- simulations was that of the initial air humidity. In the ND- case narrow cloud layer was simulated by prescribing initially relatively low ~70 % air humidity in the subcloud layer (the value of the mixing ratio near the surface was assumed to be 11 g/kg). In the D-case the relative humidity near the surface was increased upto 90% (q=13.5 g/kg). The vertical profiles of temperature and absolute humidity at different time instances (including t=0) are presented in **Figures 5 and 6**, respectively. **Figure 5** shows that vertical mixing of the BL by parcel movement leads to a change of the mean temperature profile from the initially dry adiabatic profile to the profile, in which the temperature profile tends to the moist adiabatic one within the cloud layer. As one can see (Fig. 5) the mean in ND case the depth of the cloud layer was about 370 m, while in the ND case it was about 600 m. **Figure 6** indicates that parcels' movement leads to the formation of the well mixed BL. A decrease in the mean absolute humidity above cloud base is more pronounced in the D-case and is related to the condensation of water vapor on droplets.

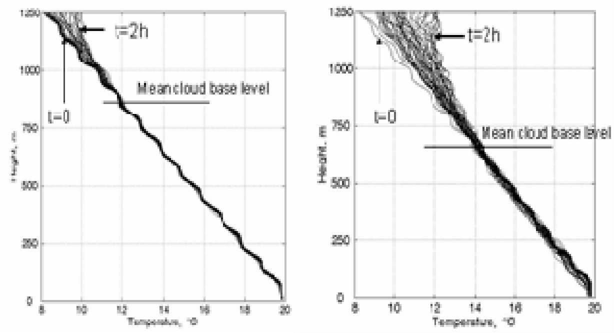

Figure 5. *The horizontally averaged profiles of temperature at different time instances in the ND (left) and D (right panel)*

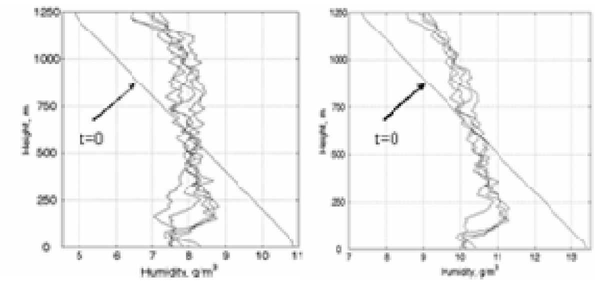

Figure 6. The same as in Figure 5, but for absolute humidity

To isolate effects of thermodynamic conditions, both dynamics and the initial CCN size distributions were assumed similar in both simulations: The total concentration of aerosols (condensation nuclei, CN) was 4650 cm^{-3}. The concentrations of nuclei with the radii r_N <0.03 μm , r_N >0.1 μm and r_N >1 μm were 4070 cm^{-3}, 130 cm^{-3} and 1 cm^{-3} , respectively. No giant CCN were assumed in the simulations. These AP parameters lead to formation of cloud parcels with droplet concentration of a few hundred of cm^{-3}.

The size distributions of dry aerosols were assumed similar in all parcels. The initial size distribution of dry CCN is shown in **Figure 7**.

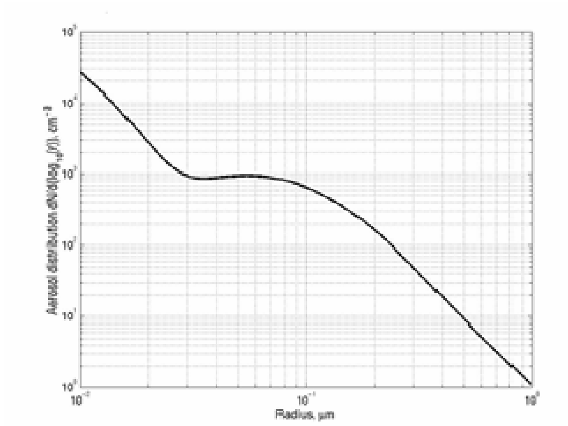

Figure 7. *Initial size distribution of dry aerosols*

The fields of radar reflectivity at t=200 min in the ND and the D cases, as well as the horizontally averaged and r.m.s. values of these quantities are shown in **Figure 8.** One can see that in ND simulation radar reflectivity is below -10 DBZ, while in the D simulation it reaches 10 DBZ in zones of intense drizzle (during the time period of drizzle fall)/ The difference in drizzle formation is caused by two factors: a) larger humidity determines higher supersaturation values and b) larger humidity determines higher cloud depths allowing more collisions during drizzle fall.

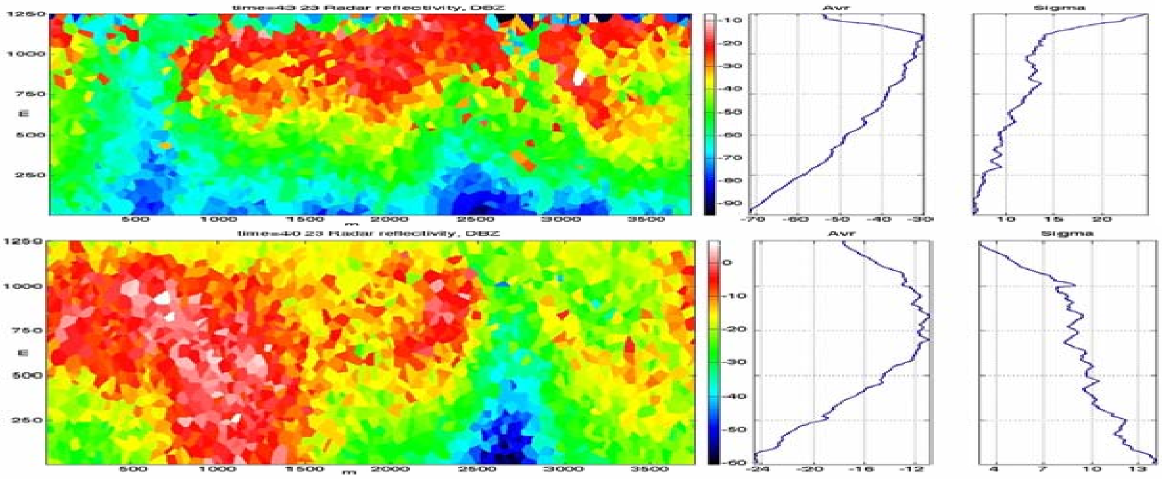

Figure 8. *Fields of radar reflectivity in the ND (upper panel) and the D cases (lower panels) at t=200 min. Horizontally averaged and r.m.s values are shown as well.*

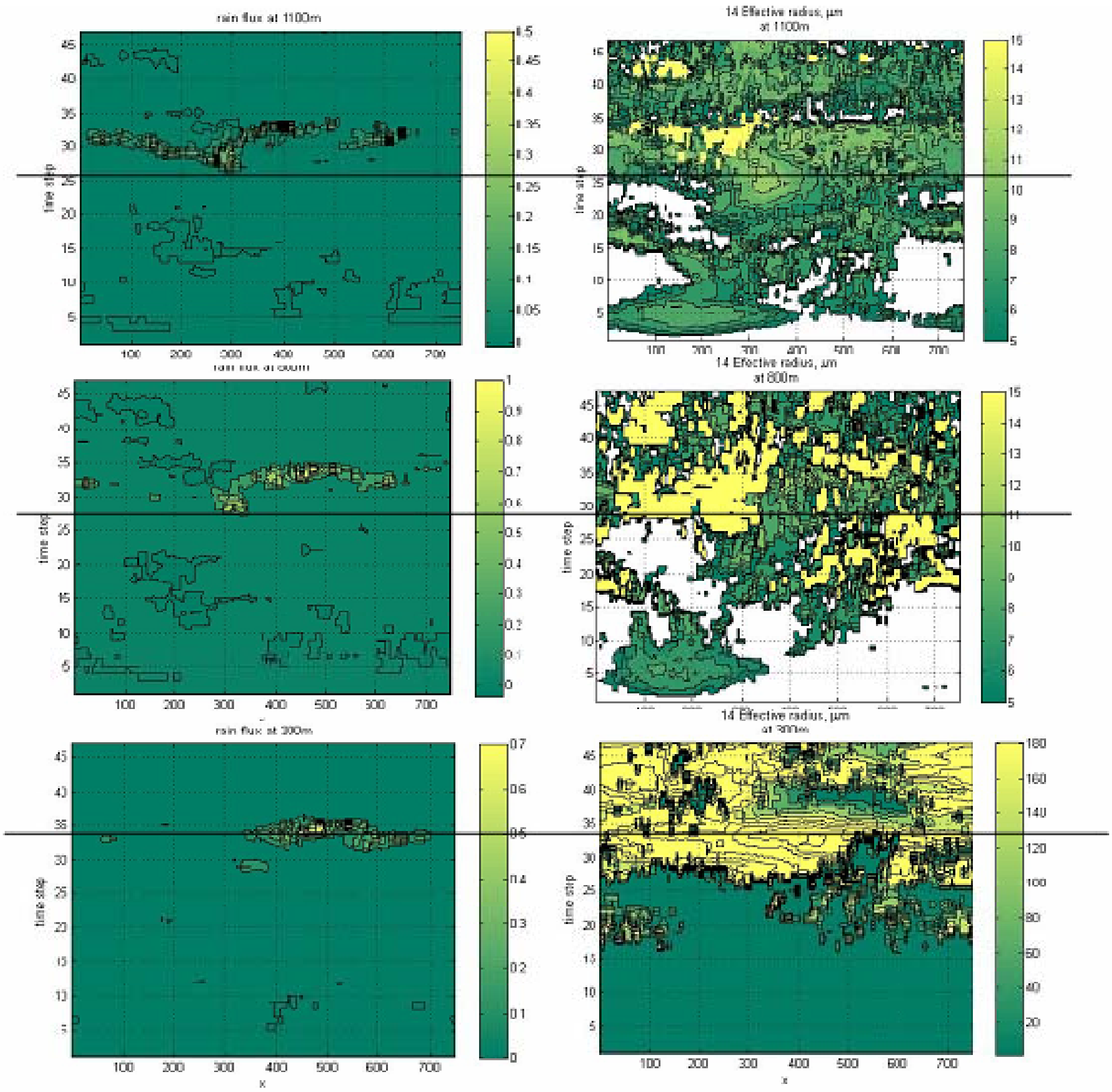

Figure 9. Time-coordinate (x) dependences of rain flux (left panels) and effective radius (right panels) at heights 1100 m (above), 800 m (middle) and 300 m (below) . Time steps are plotted with increment 5 min, and horizontal coordinate with increment 500 m.

Relationship between drizzle production in the D-simulation and the droplet spectrum width characterized here by the effective radius is illustrated in **Figure 9**. One can see that drizzle formation starts first at upper levels in the cloud when effective radius attains 8-9 μm . Then drizzle is transported by the horizontal velocity and falls through the cloud. At lower levels effective radius in drizzle increases by collisions with droplets during dizzle fall. Especially large values of effective radius at 300 m level are attributed to evaporation of small droplets, so that only largest drops attain the surface.

Figure 10 depicts diagrams of different parameters on the effective radius at t=150 min (that corresponds to time step 30 in Figure 9.

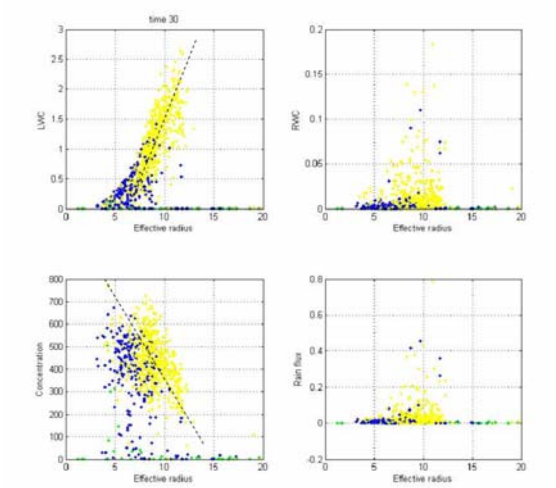

Figure 10. Scatter plot diagrams indicating relationships between CWC, droplet concentration, RWC and rainflux and the effective radius. Yellow dots indicate parcels located in the upper levels of cloud layer. Blue dots correspond to parcels located in the lower half of cloud layer. Green dots indicate parcels located below cloud base.

The tendency of the decrease in the effective radius with the increase in droplet concentration is clearly seen. In agreement with the observations, first raindrops and rainflux arises when effective radius exceeds about 8 μm .

Analysis of the results shows that raindrops form first in cloud updrafts at upper levels, where collisions begin between droplets growing by diffusion. Then drizzle particles fall in downdrafts to the lower levels. In the lower half of the cloud layer and especially, below cloud base drizzle fall within downdrafts. Thus, downdrafts related to large eddies lead to the formation of high correlation of rain flux in the vertical from the cloud top to the surface. This high correlation between location of drizzle in the vertical is a specific feature of drizzle spatial structure measured in DYCOMS-II.

The model provides a large potential for further development of remote-sensing approaches, in particular, determination of liquid water content using radar measurements.

The observed dependence (Krasnov and Russenberg 2002) (**Figure 11** (left panel**)**) indicates the existence of 3 regimes: a) linear growth of LWC with radar reflectivity Z (but with Z remaining small, so no drizzle is present), b) the second regime where Z growth significantly, while this growth does not accompanied by increase in the LWC; moreover, the decrease in LWC is often observed; c) the third regime indicates the growth of LWC with Z, but when Z is quite high indicating the existing of drizzle. Figure 11 (right panel) indicates that the model reproduces the Z-LWC diagram remarkably well.

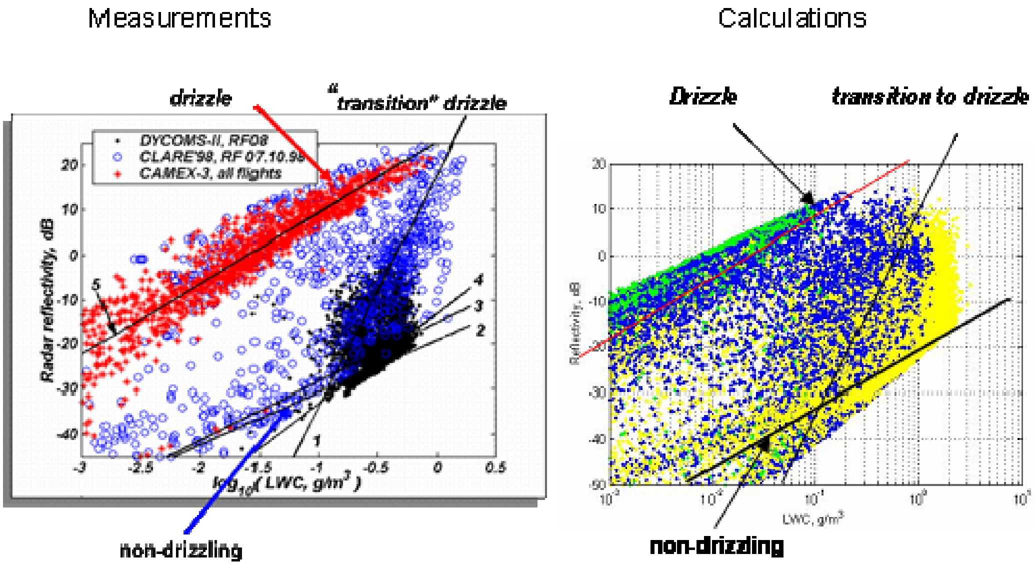

Figure 11 *The LWC-radar reflectivity relationship according to measurements (Krasnov and Russenberg 2002) (left panel), and according to calculations with the model (right panel). The model successfully reproduces the formation of the three regimes: non-drizzling, transition and drizzling ones. In the right panel yellow dots represent parcels in the upper part of cloud layer, blue dots represent parcels in the lower part of the cloud layer, and green dots represent parcels located below cloud base.*

The cloud model allows one to understand the formation of the diagram plotted in Fig. 11. **Figure 12** depicts the process of formation of the Z-LWC diagram with time. One can see that the "non-drizzling" regime forms due to diffusion growth of droplets. The transition regime starts when drizzle falling from the upper levels collect droplets of parcels located below. The third drizzle regime curve is formed at the later stage of cloud development. Parcels located near cloud base and below cloud base containing large drizzle particles contribute significantly to the formation of this regime.

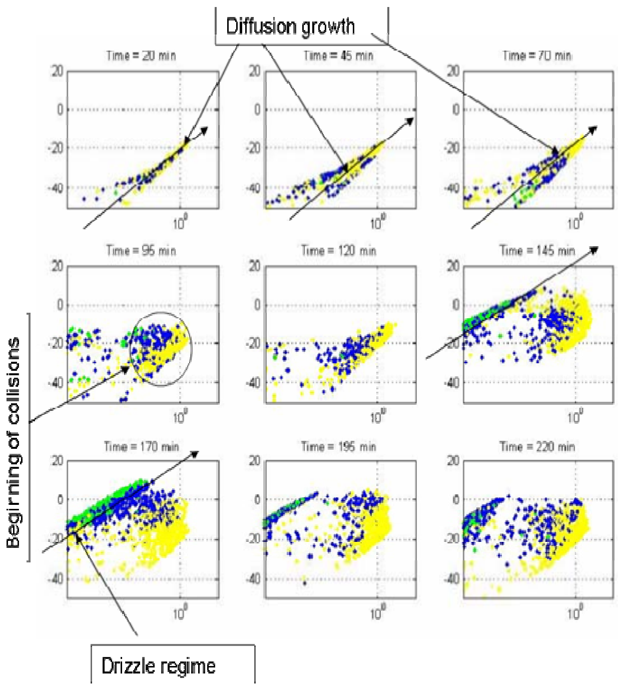

Figure 12. Time evolution of Z-LWC diagram leading to the formation of the accumulated the scattering diagram seen in Figure 11.

4. CONCLUSION

A novel trajectory ensemble model of a stratiform cloud is described. In this model the BL is fully covered by a great number of air parcels that can contain either wet AP or AP and droplets. In each parcel the microphysical processes of diffusion growth of aerosols and droplets, as well as the processes of collisions are accurately described, so that no numerical (artificial) effects influence the DSD formation. For the first time, droplet sedimentation in TEM models is described, which allows simulation of precipitation formation. The model reproduces fine features of cloud-aerosol interaction, including effects of droplet collision on the successive growth of AP in the BL. The movement of a great number of parcels provides effective vertical mixing in the BL. Thus, the processes in the cloud and subcloud layers turn out to be closely related.

The Lagrangian parcels are advected by the velocity field generated by the model of a turbulent flow obeying the preset correlation laws derived from the observations. The model calculated aerosol size distribution and the DSD, and their parameters and moments such as: concentration, cloud and rain water contents, droplet spectrum width, radar reflectivity, etc. in each parcel. Time and spatial variability of aforementioned parameters are calculated as well.

Two simulations of cloud evolution in the BL were performed. These simulations differed only by the initial humidity, which determines the difference between the cloud depths. While in the case of low humidity drizzle did not develop, in the case of high relative humidity intense drizzle develops toward t=2 h. Since the aerosol properties in both simulations were similar, the results indicate the significant role of thermodynamic factors in drizzle formation and cloud aerosol interaction.

The mechanism of drizzle formation is investigated. It is shown that drizzle start forming when effective radius exceeds about 8-9 μm. Drizzle forms first near cloud top in ascending parcels where the DSD width reaches maximal values (as compared to other parcels). Then drizzle growth by collision with cloud droplets in parcels located below.

The close relationship between drizzle flux at different height levels is demonstrated. This correlation is caused by large eddies, forming significant downdrafts from the cloud top down to the surface layer.

It is shown that the model allows one to investigate in detail the formation of the radar reflectivity- LWC scattering diagram.

The results indicate that the model simulates the cloud microphysics realistically, and, as we believe, will allow one to improve both the interpretation of remote sensing data and retrieval algorithms.

Appendix

a) *Variation of the vertical velocity.*

Taking the square of equation (1) and averaging over a great number of realizations gives:

$$\left\langle W^2 \right\rangle = \sum_{j=1}^{M}\sum_{k=1}^{N}\sum_{m=1}^{M}\sum_{n=1}^{N} \left\langle C_n D_m \left[a_m \sin\frac{2\pi mx}{L} + b_m \cos\frac{2\pi mx}{L} \right] \sin\frac{\pi nz}{H} \times C_k D_j \left[a_j \sin\frac{2\pi jx}{L} + b_j \cos\frac{2\pi jx}{L} \right] \sin\frac{\pi kz}{H} \right\rangle \qquad \text{(A1)}$$

Taking into account that coefficients $a_m(t)$ and $b_m(t)$ are non-correlated, (A1) yields:

$$\left\langle W^2 \right\rangle = \sum_{m=1}^{M} D_m^2 \left[\left\langle a_m^2 \right\rangle \left(\sin\frac{2\pi mx}{L} \right)^2 + \left\langle b_m^2 \right\rangle \left(\cos\frac{2\pi mx}{L} \right)^2 \right] \left[\sum_{n=1}^{N} C_n \sin\frac{\pi nz}{H} \right]^2 \qquad \text{(A2)}$$

The final expression is

$$\left\langle W^2 \right\rangle = \sum_{m=1}^{M} D_m^2 \left[\sum_{n=1}^{N} C_n \sin\frac{\pi nz}{H} \right]^2 \qquad \text{(A3)}$$

Analogously, one can derive an expression for horizontal velocity variation:

$$\left\langle (V - V_0)^2 \right\rangle = \left(\frac{L}{2H} \right)^2 \sum_{m=1}^{M} \left(\frac{D_m}{m} \right)^2$$
$$\left[\sum_{n=1}^{N} n C_n \cos \frac{\pi n z}{H} \right]^2 \qquad \text{(A4)}$$

b) Correlation functions of velocity components in the horizontal direction.

Multiplying the values of vertical velocity in point $\{z, x_1\}$ by the value of the vertical velocity in point $\{z, x_2\}$ and averaging the expression obtained, we get:

$$B_W = \langle W(x_1, z) W(x_2, z) \rangle = \sum_{j=1}^{M} \sum_{k=1}^{N} \sum_{m=1}^{M} \sum_{n=1}^{N}$$
$$\left\langle C_n D_m \left[a_m \sin \frac{2\pi m x_1}{L} + b_m \cos \frac{2\pi m x_1}{L} \right] \sin \frac{\pi n z}{H} \times \right. \qquad \text{(A4)}$$
$$\left. C_k D_j \left[a_j \sin \frac{2\pi j x_2}{L} + b_j \cos \frac{2\pi j x_2}{L} \right] \sin \frac{\pi k z}{H} \right\rangle$$

Using correlation relationships (2), one can simplify expression (A4) as:

$$B_W = \sum_{m=1}^{M} D_m^2$$
$$\left[\langle a_m^2 \rangle \sin \frac{2\pi m x_1}{L} \sin \frac{2\pi m x_2}{L} + \langle b_m^2 \rangle \cos \frac{2\pi m x_1}{L} \cos \frac{2\pi m x_2}{L} \right]$$
$$\left[\sum_{n=1}^{N} C_n \sin \frac{\pi n z}{H} \right]^2$$

Further simplifications result in the final expression:

$$B_W(\Delta x, z) = \left[\sum_{n=1}^{N} C_n \sin \frac{\pi n z}{H} \right]^2 \sum_{m=1}^{M} D_m^2 \cos \frac{2\pi m \Delta x}{L} \qquad \text{(A5)}$$

Analogously, the correlation function for the horizontal velocity can be written as:

$$B_V(\Delta x, z) = \left(\frac{L}{2H} \right)^2 \left[\sum_{n=1}^{N} n C_n \cos \frac{\pi n z}{H} \right]^2$$
$$\sum_{m=1}^{M} \left(\frac{D_m}{m} \right)^2 \cos \frac{2\pi m \Delta x}{L} \qquad \text{(A6)}$$

Note that B_W and B_V depend only on the distance between two points $\Delta x = x_2 - x_1$, and does not depend on the coordinates of the points themselves. Analogously, one can obtain expressions for cross-correlation functions B_{VW}. This function also depends on $\Delta x = x_2 - x_1$: $B_{VW}(x_1, x_2, z) = f(\Delta x, z)$ and is an anti-symmetrical one. The latter means that the components V and W are non-correlated in one and the same point, i.e. $B_{VW}(0, z) = 0$.

Acknowledgements

The study was performed under the support of the Israel Science Foundation (grant 173/03) and the European project ANTISTORM, as well as the Israel Ministry of Sciences (the German-Israel collaboration in Water Resources, grant WT 0403). The authors are grateful to Prof. Stevens for fruitful discussion, valuable comments and advice.

References

Albrecht, B.A., C.S. Bretherton, D. Johnson, W. Schubert, A.S. Frish, 1995: The Atlantic stratocumulus transition experiment, ASTEX. Bull. Am. Meteor.Soc., 76, 889-904.

Austin, P., Wang, Y., Pincus, R., and Kujala, V., 1995: Precipitation is stratocumulus clouds: observational and modeling results. J. Atmos. Sci., 52, 2329-2352.

Babb, D., and J. Verlinde, 1999: Vertical velocity statistics in continental stratocumulus clouds as measured by a 94 GHz radar. Geophys. Res. Lett., 26, 1177-1180.

Bott A., T. Trautmann, and W. Zdunkowski, 1996: A numerical model of the cloud-topped planetary boundary layer: radiation, turbulence and spectral microphysics in marine stratus. *Quart. J. Roy. Meteor. Soc.*, **122**, 635-667.

Bott, A., 1997: A numerical model of the cloud-topped planetary boundary layer: Impact of aerosol particles on the radiative forcing of stratiform clouds. *Quart. J. Roy. Meteor. Soc.*, **123**, 631-656.

Bott, A., 1998: A flux method for the numerical solution of the stochastic collection equation *J. Atmos. Sci.,* 55, 2284-2293.

Bott, A., 2000: A numerical model of the cloud-topped planetary boundary-layer: Influence of the physico-chemical properties of aerosol particles on the effective radius of stratiform clouds. *Atmos. Res.*, 53, 15-27.

Bower, K. N. and T.W. Choularton, 1993: Cloud processing of the cloud condensation nucleus spectrum and its climatological consequences. *Quart. J.Roy. Meteor. Soc.*, 47, 1480-1497.

Brenguier, J.L., P, Y. Chuang, Y. Fouquart, D. W. Johnson, F. Parol, H. Pawlowska, J. Pelon, L. Schuler, F. Schroder and J.R. Snider, 2000a: An overview of the AGE-2 CLOUDY COLUMN Closure Experiment. Tellus, Ser. B, 52; 814-826.

Brenguier J.-L., H. Pawlowska, L. Schuller, R. Preusker, and J. Fischer, 2000b: Radiative properties of boundary layer clouds: droplet effective radius versus number concentration. J. Atmos. Sci., 57, 803-821.

Crewell and COATHORS, 2004. The Baltex Bridge Campaign: an integrated approach for a better understanding o clouds. Bull. Amer. Meteorol. Soc., 85, 10, 1565-1584.

Duynkerke, P.G., H. Zhang, and P.J. Jonker, 1995: Microphysics and turbulent structure of nocturnal stratocumulus as observed during ASTEX. *J. Atmos. Sci.*, 52, 2763-2777.

Elliott W. P. and R. Egami (1975), CCN measurements over the ocean. *J. Atmos. Sci., 32*, 371-374.

Emanuel K. A. 1994. Atmospheric convection. *Oxford University Press.* 580pp.

Erlick C., A. Khain, M. Pinsky and Y. Segal, 2005:The effect of wind velocity fluctuations on drop spectrum broadening in stratocumulus clouds. *Atmos. Res.* 75, 15-45.

Faller A.K. and R. Keylor 1966: A numerical study of the instability of the laminar Ekman boundary layer. *J. Atmos. Sci.* 1966, 23, 466-480.

Frish, A.S., C.W. Fairall, and J. B. Snider, 1995: Measurement of stratus cloud and drizzle parameters in ASTEX with a K-band Doppler radar and a microwave radiometer. J. Atmos. Sci. 52, 2788-2799.

Feingold, G, B. Stevens, W.R. Cotton, and R.L. Walko, 1994: An explicit cloud microphysical/LES model designed to simulate the Twomey effect. Atmos. Res. 33, 207-233.

Feingold G, B., Stevens, W.R. Cotton, and A.S. Frisch, 1996: The relationship between drop in-cloud residence time and drizzle production in numerically simulated stratocumulus cloud. *J. Atmos. Sci.*, 53, 1108-1121.

Feingold, G., R.L. Walko, B. Stevens, and W.R. Cotton, 1998a: Simulation of marine stratocumulus using a new microphysical parameterization scheme. *Atmos. Res.,* 47-48, 505-528.

Feingold G., S.M. Kreidenweis and Y. Zhang 1998b: Stratocumulus processing of gases and cloud condensation nuclei. 1. Trajectory ensemble model. *J. Geophys. Res.,* 103, D16, 19,527-19,542.

Fox, N.I. and A.J. Illingworth, 1997: The retrival of stratocumulus cloud properties by ground bases cloud radar. *J. Appl. Meteor.,* 36, 465-492.

Garratt,,2000. Physics of the boundary layer of the atmosphere.

Gerber H., 1996: Microphysics of marine stratocumulus clouds with two drizzle modes. *J. Atmos. Sci*. **53,** 1649–1662.

Haralick, Robert M., L.G. Shapiro, 1991: Computer and Robot Vision, Vol. 1. Addison-Wesley, 1992

Harrington , J. Y., G. Feingold, and W.R. Cotton, 2000: Radiative impacts on the growth of a population of drops within simulated summertime arctic stratus. *J. Atmos. Sci.,* 57, 766-785.

Hobbs P. V., D. A. Bowdle and L.F. Radke (1985), Particles in the lower troposphere over the high plains of the United States. Part II: cloud condensation nuclei. *J. Clim. and Appl. Meteorol*., 24, 1358-1369

Hudson, J.G., 1993: Cloud condensational nuclei near marine cumulus. *J. Geophys. Res*., **98**, 2693-2702.

Hudson J.G., and H. Li, 1995: Microphysical contrasts in Atlantic stratus. *J. Atmos. Sci.,* 52, 3031-3040.

Hudson J.G., and S.S. Yum, 1997: Droplet spectral broadening in marine stratus. JAS, 54, 2642-2654.

Khain A. P., and M. B. Pinsky 1995 Drops' inertia and its contribution to turbulent coalescence in convective clouds: Part 1: drops' fall in the flow with random horizontal velocity, *J. Atmos. Sci.* , 52, 196-206.

Khain, A. P. and M. Pinsky, 1997: Turbulence effects on the collision kernel, Part 2: Increase of swept volume of colliding drops. *Quart. J. Roy. Meteor. Soc.,* 123, 1543-1560.

Khain, A. P., M. Ovtchinnikov, M. Pinsky, A. Pokrovsky, and H. Krugliak, 2000: Notes on the state-of-the-art numerical modeling of cloud microphysics. *Atmos. Res.* 55, 159-224.

Khain, A. D. Rosenfeld and A. Pokrovsky 2005: Aerosol impact on the dynamics and microphysics of convective clouds. *Q. J. Roy. Meteor. Soc.* 131, 2639-2663.

Khairoutdinov M.F., and Y.L. Kogan, 1999: A large eddy simulation model with explicit microphysics: validation against observations of a stratocumulus-topped boundary layer. J. Atmos. Sci., 56, 2115-2131.

Kogan Y, L., M.P. Khairoutdinov, D.K. Lilly, Z.N. Kogan and Q. Liu, 1995: Modeling of stratocumulus cloud layers in a large eddy simulation model with explicit microphysics. *J. Atmos. Sci.,* 52, 2923-2940.

Khairoutdinov ,M., and Y. Kogan, 2000: A new cloud physics parameterization n a large-eddy simulation model of maritime stratocumulus. Mon. Wea. Rev. 128, 229-243.

Khairoutdinov, M ., and D. A. Randall, 2003: Cloud resolving modeling of the ARM summer 1997IOP: Model formulation, results, uncertainties and sensitivities. J. Atmos. Sci. 60, 607-625.

Kogan Y. L. , D.K. Lilly, Z.N. Kogan, and V.V. Filyushkin, 1994: The effect of CNN regeneration on the evolution of stratocumulus cloud layers. Atmos. Res., 33, 137-150.

Kollias P., and B. Albrecht, 2000: The turbulence structure in a continental stratocumulus cloud from millimeter-wavelength radar observations. *J. Atmos. Sci.,* 57, 2417-2434.

Koren I., Y.J. Kaufmann, D. Rosenfeld, L.A. Remer, Y. Rudich, 2005: *Aerosol invigoration and restructuring of Atlantic convective clouds, GRL*, 32, L14828, doi:10.1029/2005GL023187.

Korolev, A.V., and I.P. Mazin, 1993: Zones of increased and decreased droplet concentration in stratiform clouds. *J. Appl. Meteor.,* 32, 760-773.

Korolev, A.V., 1994: A study of bimodal droplet size distributions in stratiform clouds. Atmos. Research, 32,143-170.

Korolev, A.V., 1995: The influence of suresaturation fluctuations on droplet size spectra formation. *J. Atmos. Sci.*, 52, 3620-3634.

Krasnov O., and H.W.J. Russchenberg, 2002: Use of simulations of radar and lidar data for the retrieval of microphysical parameters in low-level water clouds. 15 th Symposium on Boundary layer and turbulence, 15-19 July 2002, Wageningen, The Netherlands, AMS, 88-91

LeMone, M.A., 1990: Some observations of vertical velocity skewness in the convective planetary boundary layer. *J. Atmos. Sci.,* 47, 1163-1169.

Lenschov, D.H., J.C. Wyngaard, W.T. Pennel, 1980: Mean –field and second moment budgets in a baroclinic, convective boundary layer. *J. Atmos. Sci*. 37, 1313-1326.

Levin, Z., S. Wurzler and T. Reisin, 1998: Modification of mineral dust particles by cloud processing and subsequent effects on drop size distributions. Conference on Cloud Physics, Everett, 17-21 Aug., 504-505.

Lothon M, D. H. Lenschow, D. Leon, and G. Vali, 2004: Turbulence measurements in marine stratocumulus with airborne Doppler radar. Q. J. Roy. Met. Soc. 999, 1-19.

Martin G.M., D. W. Johnson and A. Spice (1994): The measurements and parameterization of effective radius of droplets in warm stratocumulus clouds. *J. Atmos. Sci., 51*, 1823-1842.

Mechem D. B., Y. L. Kogan, 2003: Simulating the transition from drizzling marine stratocumulus to boundary layer cumulus with a mesoscale model. *Mon. Wea. Rev*. **131**, 2342-2360.

Mason, B.J. , 1952: Production of rain and drizzle by coalescence in stratiform clouds. Q.J.R. Meteor. Soc. 78, 377-386.

Mazin, I. P., A. Kh. Khrgian, and I. M. Imyanitov, 1989: Handbook *of Clouds and Cloudy atmosphere*. Gidrometeoizdat, 647p.

Moeng, and Coathors, 1996: Simulation of a stratocumulus-topped PBL: Intercomparison among different numerical codes. Bull. Amer. Meteor. Soc., 77, 261-278.

Nicholls S. 1984: The dynamics of stratocumulus: aircraft observations and comparisons with a mixed layer model. *Quart. J. Roy. Met. Soc*., **110**, 783-820.

Nicholls,S., 1987: A model of drizzle growth in warm, turbulent, atratiform clouds. *Quart. J.Roy.Meteorol. Soc*., 113, 1141-1170.

Nicholls,S., and J.R. Leighton, 1986: An observational study of the structure of stratiform sheets. Part 1. Mean structure. *Quart. J. Roy. Met. Soc.* 112, 431-460.

Noonkester, V.R., 1984: Droplet spectra observed in marine stratus cloud layers. *J. Atmos. Sci.,* 41(5) 829-845.

O'Connor E.J. R. Hogan, A. Illingworth and J. L. Brenguier, 2004: Characteristics of drizzling and non-drizzling stratocumulus as revealed by vertical pointing cloud radar and lidar. Proc. 14th Conf. on Clouds and Precipitation. Bologna, Italy.

Pawlowska H., J.L. Brenguier, F. Burnet, 2000: Microphysical properties of stratocumulus clouds. *Atmos. Res.* 55, 15-33.

Pawlowska H., and J.L. Brenguier, 2003: An observational study of drizzle formation in stratocumulus clouds for general circulation model (GCM) parameterizations. J. Geeophys. Res. 108, 8630, doi:10.1029/2002JD002679.

Petters M.D., J. R. Snider, B. Stevens, G. Vali, I. Faloona and L. Russel, 2005: Accumulation mode aerosol, pockets of open cells, and particle nucleation in the remote subtropical Pacific marine boundary layer.???

Philippin S., E.A. Betterton, 1997: Cloud condensation nuclei concentrations in Southern Arizona: Instrumentation and early observations, *Atmos. Res. 43*, 263-275

Pinsky M. B. and A. P. Khain, 1996: Simulations of drops' fall in a homogeneous isotropic turbulence flow. *Atmosph. Research,* **40,** 223-259.

Pinsky, M., A. P. Khain, and M. Shapiro, 1999: Collisions of small drops in a turbulent flow. Pt.1 : Collision efficiency: problem formulation and preliminary results. *J. Atmos. Sci.* , 56, 2585-2600.

Pinsky, M., A.P. Khain, and M. Shapiro, 2000: Stochastic effects on cloud droplet hydrodynamic interaction in a turbulent flow. *Atmos. Res.*, 53, 131-169.

Pinsky, M., A. P. Khain, and M. Shapiro 2001: Collision efficiency of drops in a wide range of

Reynolds numbers: Effects of pressure on spectrum evolution. *J. Atmos. Sci.* 58, 742-764.
Pinsky, M., and A. Khain, 2002: Effects of in-cloud nucleation and turbulence on droplet spectrum formation. *Quart. J. Roy. Meteor. Soc.*, **128**, 501-533.
Pinsky, M. B., and A. P. Khain 2003: Fine structure of cloud droplet concentration as seen from the Fast-FSSP measurements. Part 2: Results of in-situ observations" *J. Appl. Meteor.* 42, 65-73.
Pinsky M. B., and A. P. Khain, 2004: Collisions of small drops in a turbulent flow. Part 2. Effects of flow accelerations. *J. Atmos. Sci*, 61, 1926-1939.
Pinsky M. B., A. P. Khain , B. Grits and M. Shapiro, 2005: Collisions of cloud droplets in a turbulent flow. Part 3. Relative droplet fluxes. *Atmos. Sci.* (in press)
Politovich, M. K., 1993: A study of the broadening of droplet size distribution in cumuli. *J. Atmos. Sci.*, **50**, 2230-2244.
Pruppacher, H. R., and J. D. Klett, 1997: *Microphysics of clouds and precipitation.* 2-nd edition, Oxford Press, 914 p.
Ramanathan, V., P. J. Crutzen, J. T. Kiehl and D. Rosenfeld (2001), Aerosols, climate, and the hydrological cycle, *Science, 294*, 2119-2124
Respondek, P.S., A.I. Flossmann, R.R. Alheit and H.R. Pruppacher 1995: A theoretical study of the wet removal of atmospheric pollutants: Part V. The uptake, redistribution, and deposition of (NH4)2SO4 by a convective cloud containing ice. *J. Atmos. Sci. 52*, 2121–2132.
Rogers D.P. and J.W. Telford 1986: Metastable stratus tops. *Quart. J. Roy. Met. Soc.*, 112, 481-500.
Rosenfeld D. and G. Gutman, 1994: Retrieving microphysical properties near the tops of potential rain clouds by multispectral analysis of AVHRR data. *Atmos. Res*, 34, 259-283.
Russchenberg, H.W.J. , S. Crewell, U. Loehnert, M. Quante, J. Meywerk, H. Klein Baltink, O. Krasnov, 2004: Radar observations of stratocumulus compared with in situ aircraft data and simulations. European Conference on Radar Meteorology (ERAD) 2004. Proceedings, 6-10 September, Visby, Sweden, the Netherlands, ERAD Publication series. v 2, 257-260.
Segal Y., A. Khain, and M. Pinsky and A. Sterkin, 2004: Effects of atmospheric aerosol on precipitation in cumulus clouds as seen from 2000-bin cloud parcel microphysical model: sensitivity study with cloud seeding applications. *Quart. J. Roy. Meteor. Soc. 130, 561-582.*
Segal Y. and A. Khain, 2005: Parameterization of droplet concentration for different cloud types within a wide range of aerosol conditions, *J. Geophys. Res.* (in press)
Sekiguchi, M., T. Nakajima K. Suzuki, K. Kawamoto, A. Higurashi, D. Rosenfeld, I. Sano, S. Mukai. A study of the direct and indirect effects of aerosols using global satellite datasets of aerosol and cloud parameters. *J. Geophys. Res*., 108, D22, 4699, doi: 10.1029/2002JD003359.
Slingo A., S Nicholls and J. Schmetz, 1982: Aircraft observations of marine stratocumulus during JASIN, J. R. Met.Soc., 108, 833-838
Stevens, B., G. Feingold, W. R. Cotton, and R. L. Walko, 1996: Elements of the microphysical structure of the numerically simulated nonprecipitating stratocumulus. *J. Atmos. Sci.,* **53**, 980-1006.
Stevens, B, W.R. Cotton, G. Feingold, and C. Moeng, 1998: Large eddy simulations of strongly precipitating, shallow, stratocumulus-topped boundary layers. J. Atmos. Sci. 55, 3616-3638.
Stevens, B, C.H. Moeng and P.P. Sullivan 1999: Large-eddy simulations of radaitively driven convection: Sensitivities to the representation of small scales. J. Atmos. Sci. 56, 3963-3984.
Stevens, B, and Coauthors, 2003a: Dynamics and Chemistry of maritime stratocumulus-DYCOMS-II. Bull. Amer. Meteorol. Soc. 84, 579-593.
Stevens, B, and Coauthors, 2003b, On entrainment rates in nocturnal maritime stratocumulus. Quart. J. Roy. Meteorol. Soc. 129, 3469-3492.

Stevens, B, G. Vali, K. Comstock, R. Wood, M.C. vanZanten; P.H. Austin, C. S. Bretherton, and D.H. Lenshow, 2005: Pockets of open cells (POCs) and drizzle in marine stratocumulus. Bull. Amer. Meteorol. Soc., 51-57

Telford J.W. and T.S. Keck (1988): Atmospheric structure generated by entrainment into clouds. *Atmos. Res*. 202, 191-216.

Twohy, C.H, M.D Petters, J. R. Snider, B. Stevens, W. Tahnk, M. Wetzel, L. Russell, and F. Burnet, 2005, J. Geophys. Res 110, D08203, doi: 10.1029/2004JD005116

Twomey S., 1977: The influence of pollution on the shortwave albedo of clouds. *Journal of Atmospheric Sciences*, **34**, 1149-1154.

VanZanten M. C., B. Stevens, G. Vali, D. H. Lenschow, 2005: Observations in nocturnal marine stratocumulus. *J. Atmos. Sci*., **62**, 88-106.

VanZanten M. C., and B. Stevens 2005: On the observed structure of heavily precipitating maritme stratocumulus J. Atmos. Sci (in press)

Wolf, D.A. H.W.J. Russchenberg , L.P. Ligthart, 2000: Radar reflection from clouds: Gigahertz backscatter cross sections and Doppler spectra. IEEE Trans. Ant Prop., v. 48, 254-259.

Yum, S.S. and J.G. Hudson (2002): Maritime/continental microphysical contrasts in stratus. Tellus, Se. B, 54, 61-73.

Zhelnin A. A. and A. P. Khain, 1975: On account for moisture in calculating the height of the convective layer. *Meteorology and Hydrology,* N2, 44-47.